Inorg. Chem. **2004**, *43*, 747−756

Does α-Fluorination Affect the Structural *trans*-Influence and Kinetic *trans*-Effect of an Alkyl Ligand? Molecular Structures of $Pd(TMEDA)(CH_3)(R_F)$ and a Kinetic Study of the *trans* to *cis* Isomerization of $Pt(TMEDA)(CH_3)_2I(R_F)$ [$R_F = CF_2CF_3$, $CFHCF_3$, CH_2CF_3]

Russell P. Hughes,*,† Monique A. Meyer,† Mark D. Tawa,† Antony J. Ward,† Alex Williamson,† Arnold L. Rheingold,‡ and Lev N. Zakharov‡

Department of Chemistry, 6128 Burke Laboratory, Dartmouth College, Hanover, New Hampshire 03755, and Department of Chemistry and Biochemistry, University of California, San Diego, California 92093-0358

Received August 11, 2003

Reaction of $Pd(TMEDA)(CH_3)_2$ [TMEDA = tetramethylethylenediamine] with fluoroalkyl iodides R_FI affords a series of square planar Pd(II) complexes $Pd(TMEDA)(CH_3)(R_F)$ [$R_F = CF_2CF_3$ (**9**), $CFHCF_3$ (**10**), CH_2CF_3 (**11**)], presumably by oxidative addition followed by reductive elimination of CH_3I. The solid-state structures of each compound have been determined by single crystal X-ray diffraction studies, allowing the effect of increasing α-fluorination on the structural *trans*-influence of alkyl ligands to be examined. In these compounds there is no significant difference observed in the *trans*-influence of the three fluorinated alkyl ligands toward the *trans*-N atom, although a significant *cis*-influence on the neighboring methyl ligand is apparent. Oxidative addition of the same series of fluoroalkyl ligands to the corresponding $Pt(TMEDA)(CH_3)_2$ affords octahedral Pt(IV) complexes *trans*-$Pt(TMEDA)(CH_3)_2(R_F)I$ [$R_F = CF_2CF_3$ (**12**), $CFHCF_3$ (**13**), CH_2CF_3 (**14**)] as the kinetic products. In each case, subsequent isomerization to the corresponding all *cis*-isomers is observed; in the case of **13,** the stereocenter at the α-carbon results in two diastereomeric *cis*-isomers, which are formed at different rates. The molecular structures of **13** and its more stable all *cis*-isomer **16b** have been crystallographically determined. Kinetic studies of the *trans*–*cis* isomerization reactions show the mechanism to involve a polar transition state, presumably involving iodide dissociation, followed by rearrangement of the cation, and iodide recombination. High dielectric solvents increase the rate, but solvent coordinating ability has no effect. Dissolved salts (LiI, LiOTf) show normal accelerative salt effects, with no inhibition in the case of added iodide, consistent with the formation of an intimate ion pair intermediate. The kinetic parameters show that the *trans*-effects of fluoroalkyl ligands in these compounds follow the order expected from the relative σ-donor properties of the ligands, with $CF_2CF_3 < CFHCF_3 < CH_2CF_3$.

Introduction

Relative thermodynamic *trans*-influences and kinetic *trans*-effects[1−3] are commonly invoked to rationalize the effects of certain ligands on the structural parameters and/or substitutional lability of other ligands *trans* to themselves and, as such, justify their coverage in most inorganic chemistry texts.[4] For a number of years we have been interested in the comparative chemistry of alkyl and fluoroalkyl ligands and the effects of fluorination on the chemical nature of the metal−carbon bond.[5−12] As a result, the effect of fluorination

* To whom correspondence should be addressed. E-mail: rph@dartmouth.edu. Fax: (603) 646-3946.
† Dartmouth College.
‡ University of California, San Diego.

(1) Pidcock, A.; Richards, R. E.; Venanzi, L. M. *J. Chem. Soc. A* **1966**, 1707−1710.
(2) Appleton, T. G.; Clark, H. C.; Manzer, L. E. *Coord. Chem. Rev.* **1973**, *10*, 335−422.
(3) Atwood, J. D. *Inorganic and organometallic reaction mechanisms*, 2nd ed.; VCH Publishers: New York, 1997.
(4) *Inorganic chemistry*, 3rd ed.; Shriver, D. F., Atkins, P. W., Eds.; W. H. Freeman and Co.: New York, 1999.
(5) Blanchard, M. D.; Hughes, R. P.; Concolino, T. E.; Rheingold, A. L. *Chem. Mater.* **2000**, *12*, 1604−1610.
(6) Richardson, D. E.; Lang, L.; Eyler, J. R.; Kircus, S. R.; Zheng, X.; Morse, C. A.; Hughes, R. P. *Organometallics* **1997**, *16*, 149−150.
(7) Lichtenberger, D. L.; Elkadi, Y.; Gruhn, N. E.; Hughes, R. P.; Curnow, O. J.; Zheng, X. *Organometallics* **1997**, *16*, 5209−5217.
(8) Hughes, R. P.; Overby, J. S.; Williamson, A.; Lam, K.-C.; Concolino, T. E.; Rheingold, A. L. *Organometallics* **2000**, *19*, 5190−5201.
(9) Hughes, R. P.; Smith, J. M.; Liable-Sands, L. M.; Concolino, T. E.; Lam, K.-C.; Incarvito, C.; Rheingold, A. L. *J. Chem. Soc., Dalton Trans.* **2000**, 873−879.
(10) Bowden, A. A.; Hughes, R. P.; Lindner, D. C.; Incarvito, C. D.; Liable-Sands, L. M.; Rheingold, A. L. *J. Chem. Soc., Dalton Trans.* **2002**, 3245−3252.

10.1021/ic030251j CCC: $27.50 © 2004 American Chemical Society
Published on Web 12/30/2003

Chart 1

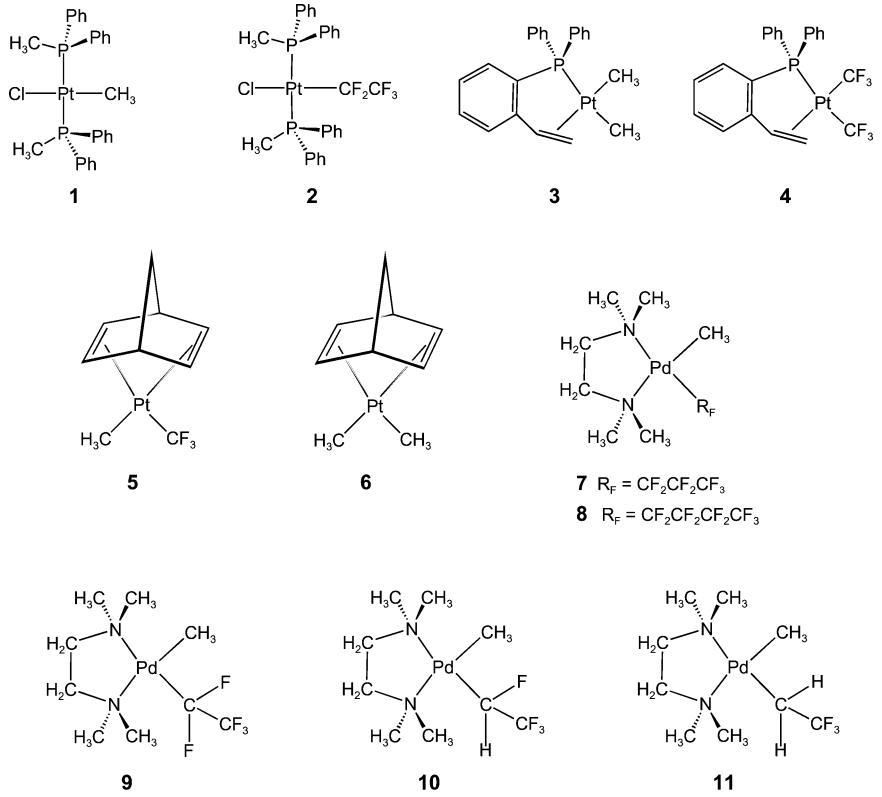

on the relative *trans*-influence and *trans*-effect of alkyl ligands has been of logical interest to us.[8]

The *trans*-Influence. The relative *trans*-influences of ligands in square planar Pd(II) and Pt(II) compounds has been the subject of extensive study and review,[2] and over the past 40 years, a number of studies of the *trans*-influences of CF_3 and CH_3 ligands have appeared. In general, the relative *trans*-influences have been determined spectroscopically rather than crystallographically. However, in an attempt to make the clearest possible structural comparison, the structures of Pt complexes **1** and **2** were determined (Chart 1); the CF_3 analogue of **2** exhibited structural disorder between Cl and CF_3, precluding any meaningful comparison with **1**.[13] The conclusion of this study was that CH_3 has a significantly longer bond to Pt (Pt−C = 2.081(6) Å) in **1** than does C_2F_5 in **2** (Pt−C = 2.002(9) Å), but it has a higher *trans*-influence toward Cl (Pt−Cl = 2.412(2) Å) than does C_2F_5 (Pt−Cl = 2.363(2) Å). The Pt−Cl bond in **2** (and its CF_3 analogue) was also shown to be stronger than that in **1** by the values of ν_{Pt-Cl} in **1** (272 cm^{-1}) and **2** (302 cm^{-1}). In this case the shorter, and supposedly stronger, bond to the fluorinated carbon atom clearly results in a stronger, shorter bond to the *trans*-Cl.[13] This comparison was complemented by a second structural study of complexes **3** and **4**, each of which contains a pair of Pt−C bonds *trans* to potentially π-accepting phosphorus and alkene ligands.[14] In these compounds, the Pt−CH_3 bond lengths in **3** (2.1665(5)Å *trans* to P; 2.052(6) Å *trans* to vinyl) are longer than the Pt−CF_3 distances in **4** (2.082(5) Å trans to P; 2.032(5) Å trans to vinyl), but the corresponding Pt−P (2.276(1) Å) and Pt−alkene (2.223(5) and 2.201(5) Å) bonds in **3** are shorter than the Pt−P (2.310(1) Å) and Pt−alkene (2.290(5) and 2.245(5) Å) bonds in **4**. Consequently, the structural *trans*-influences of CH_3 and CF_3 in these compounds appear to be reversed from those in **1** and **2**. One explanation for both sets of data would be that CF_3 is capable of being a π-acceptor ligand, increasing π-donation from chloride in **2** to strengthen the bond trans to itself and competing with the other π-acceptors in **3** and **4** to weaken their respective bonds to Pt.[14] However, the idea that CF_3 can act as a significant π-acceptor ligand has fallen into disfavor after MO calculations by Fenske and Hall indicated that this bonding component was of no significance in $(CF_3)Mn(CO)_5$.[15] In addition, a much more recent valence bond approach to bonding in transition metal complexes has suggested that the *trans*-influence may exclusively be attributable to σ-effects.[16] The only previous example of a structure in which it would be possible to obtain an intramolecular comparison of methyl and trifluoromethyl ligands *trans* to the same ligand in the same complex is **5**.[17] Unfortunately, the structures of **5** and its dimethyl analogue **6** could not be accurately determined, and the values of all the Pt−alkyl distances in both compounds are indistinguish-

(11) Johnston, B. F.; Rankin, D. W. H.; Robertson, H. E.; Hughes, R. P.; Lomprey, J. R. *Organometallics* **2002**, *21*, 4840−4846.
(12) Hughes, R. P. *Adv. Organomet. Chem.* **1990**, *31*, 183−267.
(13) Bennett, M. A.; Chee, H.-K.; Robertson, G. B. *Inorg. Chem.* **1979**, *18*, 1061−1070.
(14) Bennett, M. A.; Chee, H.-K.; Jeffery, J. C.; Robertson, G. B. *Inorg. Chem.* **1979**, *18*, 1071−1076.
(15) Hall, M. B.; Fenske, R. F. *Inorg. Chem.* **1972**, *11*, 768−775.
(16) Landis, C. R.; Firman, T. K.; Root, D. M.; Cleveland, T. *J. Am. Chem. Soc.* **1998**, *120*, 1842−1854.

able at approximately 2.07(2) Å; likewise, all the Pt−alkene distances exhibit insignificant differences.

In an attempt to remove all issues relating to the π-properties of the ancillary ligands, we prepared the methyl(fluoroalkyl) complexes **7** and **8**, containing the tetramethylethylenediamine (TMEDA) ligand, and determined their molecular structures by X-ray crystallography.[8] We reasoned that these structures would allow a direct intramolecular comparison between the *trans*-influences of methyl and fluoroalkyl ligands in a system in which the alkyl and fluoroalkyl ligands are each *trans* to the same ligand, and any differences in bond lengths derived from electronic effects in such complexes must be predominantly, if not exclusively, due to σ-effects. The conclusion was that if the Pd−N bond lengths are used to determine the relative *trans*-influences of the fluoroalkyl and methyl ligands, the expected trend of methyl > fluoroalkyl is followed.[2] Relative to the CH_3 ligand, the shorter Pd−R_F bond has a shorter Pd−N bond *trans* to it. The conclusion that R_F possesses a smaller structural *trans*-influence than CH_3 in these compounds parallels the results of Bennett on compounds **1** and **2**, and contrast, as do his results, with the structural *trans*-influences obtained for **3** and **4**.

The *trans*-Effect. The kinetic *trans*-effect has been most commonly studied in substitution reactions of square planar d^8 platinum(II) complexes. Clearly, it is not a separate issue from the *trans*-influence, as ligands that have high *trans*-influences also have high *trans*-effects by weakening the bond to the *trans*-ligand and increasing the rate of substitution.[3,4]

The most widely studied system involves substitution in square planar d^8 platinum(II) complexes. Good σ-donor ligands have high *trans*-effects by contributing more electron density to the shared orbital between itself and the *trans*-ligand, thereby weakening the bond to the leaving group.[3] However, in associative substitution reactions in which electron density at the metal center is increasing in the transition state leading to the 5-coordinate intermediate, good π-acceptor ligands also have understandably high *trans*-effects.[3]

Perhaps due to the higher reactivity and lower stereochemical complexity of substitution reactions in square-planar complexes compared to octahedral complexes, relatively little effort has been put forth in the examination of kinetic *trans*-effects in the latter systems.[18−20] From work published on the kinetic *trans*-effect in ligand substitution for Co(II), Pt(IV), Cr(0), Fe(II), Ru(II), Rh(III), and Ir(III) complexes, it is believed in general that most octahedral complexes undergo dissociative ligand substitution, characterized by first-order kinetic rate laws.[18−20] Studies of substitution reactions of *trans*-Cr(CO)$_4$LL′ showed poor correlation between the structural *trans*-influence and the kinetic *trans*-effect, indicating that stabilization of the transition-state leading to the dissociatively formed 5-coordinate intermediate is more important in determining the kinetic *trans*-effect of a given ligand.[21] The *trans*-effect order of PPh_3 > $P(OPh)_3$, $P(OMe)_3$ > CO was found to be the same for different leaving groups, suggesting that the *trans*-effect arises by a stabilization of the unsaturated 5-coordinate intermediate by strongly donating ligands.[21] This effect should be accentuated if the intermediate is a cation, formed by dissociation of an anionic ligand.[21] Consequently, observation of different kinetic *trans*-effects in octahedral systems should provide an unambiguous test of the relative σ-donor abilities of different alkyl ligands, but there does not appear to be any published work on the kinetic *trans*-effect of alkyl versus fluoroalkyl ligands on the rate of ligand substitution in octahedral compounds.

As described above, recent studies of palladium and platinum compounds containing the TMEDA ligand support the idea that fluoroalkyl ligands have a smaller *trans*-influence than the analogous alkyl ligands,[8,22] and follow the prediction made on the basis of the relative σ-donor capabilities of the ligands.

With confirming information in hand regarding the overall effects of perfluorination on the *trans*-influences of alkyl ligands, we turned to a systematic evaluation of the effects of successive α-fluorination on both the *trans*-influences and *trans*-effects of alkyl ligands. The results are reported here.

Results and Discussion

Effect of α−Fluorination on the Structural *trans*-Influence of Alkyl Ligands. Our initial targets for structural studies were the three compounds **9**−**11**, containing CF_2CF_3, $CFHCF_3$, and CH_2CF_3 ligands, respectively. The synthesis of this series of TMEDA complexes was straightforward using the methodology previously described for analogous fluoroalkyl(methyl) complexes.[8] Reaction of Pd(TMEDA)$(CH_3)_2$ with the appropriate fluoroalkyl iodide in hexanes solution afforded typically 45−55% yields of the products, presumably via oxidative addition of the fluoroalkyl iodide to give a Pd(IV) intermediate, followed by reductive elimination of CH_3I. The iodo(methyl) complex Pd(TMEDA)(CH_3)I is also formed, and as described previously, choice of solvent is important in this reaction.[8] Platinum(IV) analogues of the putative Pd(IV) intermediates have been isolated previously;[22] their structures and isomerization reactions are discussed in more detail later in this paper.

All three compounds **9**−**11** have been characterized in the solid state by single crystal X-ray diffraction studies. ORTEP diagrams for each structure are provided in Figures 1−3, with details of the structural determinations presented in Table 1. Figure 4 gives a pictorial comparison of selected bond lengths and angles for these three structures.

(17) Appleton, T. G.; Hall, J. R.; Kennard, C. H. L.; Mathieson, M. T.; Neale, D. W.; Smith, G.; Mak, T. C. W. *J. Organomet. Chem.* **1993**, *453*, 299−306.
(18) Coe, B. J.; Glenwright, S. J. *Coord. Chem. Rev.* **2000**, *203*, 5−80.
(19) Flood, T. C.; Lim, J. K.; Deming, M. A. *Organometallics* **2000**, *19*, 2310−2317.
(20) Flood, T. C.; Lim, J. K.; Deming, M. A.; Keung, W. *Organometallics* **2000**, *19*, 1166−1174.
(21) Wovkulich, M. J.; Atwood, J. D. *Organometallics* **1982**, *1*, 1316−1321.
(22) Hughes, R. P.; Sweetser, J. T.; Tawa, M. D.; Williamson, A.; Incarvito, C. D.; Rhatigan, B.; Rheingold, A. L.; Rossi, G. *Organometallics* **2001**, *20*, 3800−3810.

Table 1. Crystal Data, Data Collection, and Refinement Parameters

	9	**10**	**11**	**13**	**16b**
formula	$C_9H_{19}F_5N_2Pd$	$C_9H_{20}F_4N_2Pd$	$C_9H_{21}F_3N_2Pd$	$C_{10}H_{23}F_4IN_2Pt$	$C_{10}H_{23}F_4IN_2Pt$
fw	356.66	338.67	320.68	569.29	569.29
space group	$P2_1/n$	$P2_1/n$	$P2_1/n$	$P2_1/n$	$Pbca$
a, Å	11.7095(10)	8.5809(6)	8.4893(8)	7.6782(3)	13.9073(9)
b, Å	8.7214(7)	11.1727(7)	11.1928(11)	14.1324(6)	14.3578(9)
c, Å	13.8253(11)	13.9548(9)	13.7890(13)	14.3382(6)	15.9653(11)
α, deg					
β, deg	106.942(2)	104.240(1)	105.053(2)	97.661(1)	
γ, deg					
V, Å^3	1350.61(19)	1296.76(15)	1265.3(2)	1541.97(11)	3187.9(4)
Z, Z'	4, 1	4, 1	4, 1	4, 1	8, 1
cryst color, habit	yellow, plate	colorless, block	colorless, block	colorless, tablet	colorless, block
D(calc), g cm^{-3}	1.754	1.735	1.683	2.452	2.372
μ(Mo Kα), mm^{-1}	1.413	1.456	1.476	11.13	10.767
temp, K	173(2)	173(2)	173(2)	120(2)	223(2)
diffractometer[a]	Siemens P4/CCD	Siemens P4/CCD	Siemens P4/CCD	Bruker Smart Apex CCD	Siemens P4/CCD
reflns indep	2284 [R_{int} = 0.0292]	2685 [R_{int} = 0.0217]	2324 [R_{int} = 0.0240]	3602 [R_{int} = 0.0228]	2291 [R_{int} = 0.0416]
$R(F)$,[a] %	3.46	2.82	3.00	2.75	2.18
$R(wF^2)$,[b] %	9.47	7.28	10.93	7.61	5.88

[a] Radiation: Mo K$^{\alpha}$ (λ = 0.71073). [a] $R = \sum||F_o| - |F_c||/\sum|F_o|$. [b] $R(wF^2)=\{\sum[w(F_o^2 - F_c^2)^2]/\sum[w(F_o^2)^2]\}^{1/2}$; $w = 1/[\sigma^2(F_o^2) + (aP)^2 + bP]$, $P = [2F_c^2 + \max(F_o, 0)]/3$.

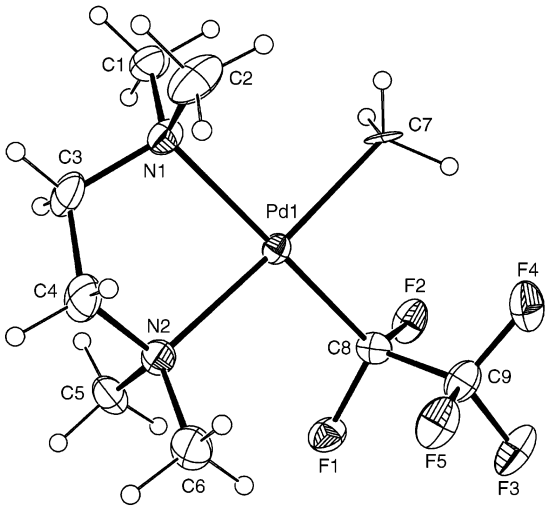

Figure 1. ORTEP diagram of **9**, showing the atom labeling scheme. Thermal ellipsoids are shown at 30% probability.

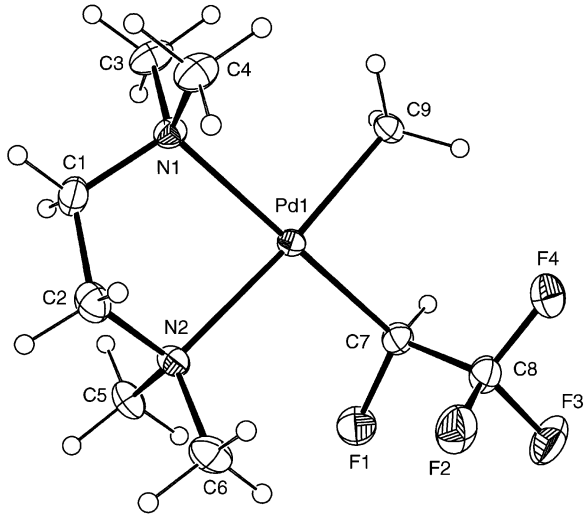

Figure 2. ORTEP diagram of **10**, showing the atom labeling scheme. Thermal ellipsoids are shown at 30% probability.

The solid-state structures of the three complexes are remarkably similar in terms of the basic conformations of the ligands. The fluoroalkyl ligand adopts a conformation

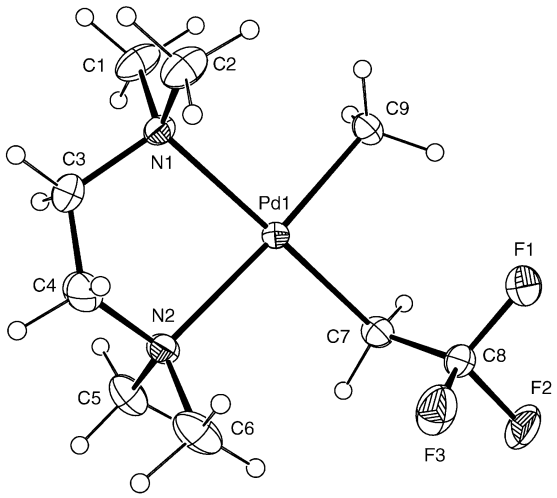

Figure 3. ORTEP diagram of **11**, showing the atom labeling scheme. Thermal ellipsoids are shown at 30% probability.

in which the β-CF_3 is almost perpendicular to the coordination plane, with torsional angles $CH_3-Pd-C_\alpha-C_\beta$ of 79.5° (**9**), 88.1° (**10**), and 85.3° (**11**). The sense of the TMEDA ring pucker is identical in all three compounds and avoids eclipsing between the β-CF_3 and methyls on the *cis*-N. These conformational preferences have been noted for analogues **7** and **8**, and a detailed rationale has been provided previously.[8] The essentially identical angles between the ligated atoms can be noted in Figure 4, as can the identical bond angle between $Pd-C_\alpha-C_\beta$ in each complex. It seems fair to conclude that there are no significantly different steric forces at play in this series of compounds. The Pd−N distances *trans* to CH_3 are identical within experimental error, as are those *trans* to R_F, although the former are all significantly longer than the latter. On the basis of this criterion, we can conclude that there is no difference in the structural *trans*-influence of an 2,2,2-trifluoroethyl ligand as the degree of α-fluorination is changed.

As expected, the $Pd-R_F$ distances are significantly shorter than the corresponding $Pd-CH_3$ distances in **9** and **10**, but the $Pd-CH_2CF_3$ and $Pd-CH_3$ distances in **11** are identical within experimental error. The α-fluorination clearly does

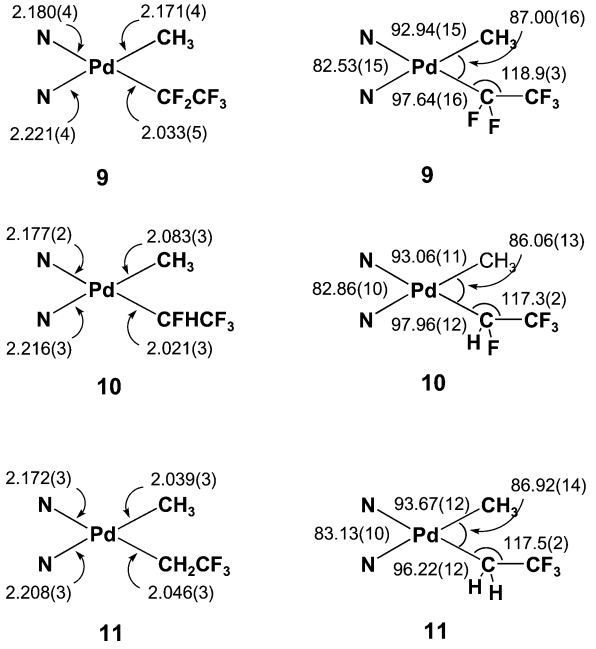

Figure 4. Pictorial comparison of bond lengths (Å) and angles (deg) for complexes **9**−**11**.

affect the Pd−R$_F$ bond length, although it is not possible to distinguish a meaningful difference between this parameter in **9** and **10**. It should be noted that any differences in s-character of the C orbital used to bind to Pd induced by α-fluorination are not reflected in the Pd−C$_\alpha$−C$_\beta$ bond angle, which is identical for all three compounds. Curiously, the most dramatic structural difference between the three compounds lies in the Pd−CH$_3$ distances. As the number of α-fluorines on the *cis*-alkyl ligand increases, there is a significant lengthening of the Pd−CH$_3$ bond. As noted above, this change is not accompanied by significant changes in bond angles within the coordination sphere, or any change in the distance from Pd the corresponding *cis*-N. Consequently, it is tempting to ascribe differences between alkyl and fluoroalkyl ligands in these systems as involving a structural *cis*- rather than a *trans*-influence, with steric effects dominating and the response to steric stress being bond elongation rather than angle distortion. Perhaps not surprisingly, the monodentate CH$_3$ ligand appears to be far more flexible in adjusting its distance to the metal than the N atoms of the chelate diamine ligand.

While all three compounds have been characterized by X-ray diffraction (see above), their solution structures have also been confirmed by NMR spectroscopy and show some interesting features. The ^{1}H NMR spectrum for **9** is straightforward, with the metal bound methyl group appearing as an apparent sextet at δ 0.67 ppm (J_{HF} = 1 Hz). The observed sextet is actually an overlapping triplet of quartets, due to equivalent coupling to both the CF$_2$ and CF$_3$ groups. There are two resonances at δ 1.65 and 2.09 ppm assigned to the two TMEDA methyl groups in **9** while the methylene units appear as a complex multiplet clustered at δ 1.40 ppm. The ^{19}F NMR spectrum shows two apparent singlets at δ −97.8 ppm for the CF$_2$ group and δ −80.9 ppm for CF$_3$. The small ^{1}H−^{19}F coupling observed in the ^{1}H spectrum is not observable in the ^{19}F spectrum, and significant vicinal ^{19}F−^{19}F coupling is not observed, as expected.[23]

Compound **11** shows the expected five resonances in the ^{1}H NMR spectrum, with the CF$_3$CH$_2$ protons observed as a quartet at δ 1.60 ppm (J_{HF} = 17 Hz) due to coupling to the CF$_3$ group. The ^{19}F NMR spectrum shows the expected triplet at δ −47.3 ppm (J_{FH} = 17 Hz) for the CF$_3$ group.

The ^{1}H NMR spectrum for **10** is more complicated due to the presence of the stereocenter at the α-carbon of the ethyl ligand, as well as the additional ^{1}H−^{19}F coupling in the CF$_3$-CFH ligand. The palladium methyl group again shows coupling with fluorine as it does for **9**, but the peak is a quartet (J_{HF} = 1 Hz) from coupling with only the CF$_3$. Unlike **9** and **11**, the TMEDA methyl groups appear as four distinct resonances due to the lack of symmetry in the molecule. The α-proton of the CF$_3$CFH ligand appears as a doublet of quartets at δ 6.01 ppm with a large geminal coupling to the α-fluorine (J_{HF} = 50 Hz) and coupling to CF$_3$ (J_{HF} = 13 Hz). The α-fluorine resonance is observed upfield at δ −220.0 ppm as a doublet of quartets (J_{FH} = 50 Hz, J_{FF} = 13 Hz) in the ^{19}F NMR spectrum, and the CF$_3$ resonates as an apparent triplet at δ −67.9 ppm due to equivalent coupling with both the α-proton and α-fluorine (J_{FF} = J_{FH} = 13 Hz).

Effect of α-Fluorination on the Kinetic *trans*-Effect of Alkyl Ligands. While the formation of Pd(II) compounds by oxidative addition of fluoroalkyl iodides to Pd(TMEDA)-(CH$_3$)$_2$ undoubtedly proceeds via an octahedral Pd(IV) intermediate, followed by reductive elimination of CH$_3$I, this intermediate has not been observed or isolated. However, we have previously reported that similar oxidative addition reactions to the corresponding platinum precursor do result in isolable Pt(IV) fluoroalkyl species.[22] Our previous synthetic procedures yielded only the *cis*-isomers,[22] but we subsequently observed that at low temperatures the corresponding *trans*-isomers could be isolated, and the rates of their subsequent isomerization to the *cis*-isomers monitored.

Three compounds **12**−**14** were synthesized by oxidative addition of fluoroalkyl iodides to a toluene suspension of Pt(TMEDA)(CH$_3$)$_2$ at −78 °C. When the solvent was removed in vacuo below 0 °C the final product in each case was that in which the R$_F$−I bond had added in a *trans*-fashion (hereafter referred to as the *trans*-isomer). Use of more polar solvents, like methylene chloride, and carrying out the reaction at room temperature, affords the corresponding isomers in which the R$_F$ and I ligands were *cis*, while maintaining the *cis* relationship between the methyl groups (hereafter referred to as the *cis* isomers, **15**−**17**). Even in toluene or benzene solution the *trans* compounds readily isomerize to their *cis* isomers at room temperature, confirming that the *trans* complex is the kinetic product of oxidative addition, as is usually found for oxidative addition to Pt(II) precursors.[24−31]

(23) Schorn, C.; Naumann, D.; Scherer, H.; Hahn, J. *J. Fluorine Chem.* **2001**, *107*, 159−169.
(24) Baar, C. R.; Jenkins, H. A.; Vittal, J. J.; Yap, G. P. A.; Puddephatt, R. J. *Organometallics* **1998**, *17*, 2805−2818.
(25) Levy, C. J.; Puddephatt, R. J. *J. Am. Chem. Soc.* **1997**, *119*, 10127−10136.

Table 2. First-Order Rate Constants (s^{-1}) for *trans*−*cis* Isomerization at 21 °C

solvent	12 → 15 ($R_F = CF_2CF_3$)	14 → 17 ($R_F = CH_2CF_3$)	13 → 16 ($R_F = CFHCF_3$)
C_6D_6	$k_1 = 1.69(\pm0.06) \times 10^{-5}$ $k_{-1} = 9.37(\pm0.36) \times 10^{-7}$	$k_1 = 5.97(\pm0.54) \times 10^{-5}$ $k_{-1} = 2.69(\pm0.24) \times 10^{-6}$	$k_1 = 1.96(\pm0.02) \times 10^{-5}$ $k_{-1} = 6.17(\pm0.06) \times 10^{-6}$ $k_2 = 5.87(\pm0.47) \times 10^{-6}$ $k_{-2} = 3.75(\pm0.30) \times 10^{-7}$ $k_3 = 6.42(\pm0.20) \times 10^{-6}$ $k_{-3} = 1.29(\pm0.20) \times 10^{-7}$
DMF-d_7	too fast to measure		
CD_3NO_2	too fast to measure		
$(CD_3)_2CO$	$k_1 = 2.74(\pm0.01) \times 10^{-4}$ k_{-1} = small[a]	$k_1 = 6.80(\pm0.25) \times 10^{-4}$ $k_{-1} = 4.25(\pm0.16) \times 10^{-5}$	
0.10 M LiI in $(CD_3)_2CO$	$k_1 = 3.43(\pm0.06) \times 10^{-4}$ k_{-1} = small[a]	$k_1 = 6.27(\pm0.31) \times 10^{-4}$ $k_{-1} = 7.37(\pm0.36) \times 10^{-5}$	
0.20 M LiI in $(CD_3)_2CO$	$k_1 = 4.06(\pm0.02) \times 10^{-4}$ k_{-1} = small[a]	$k_1 = 7.88(\pm0.41) \times 10^{-4}$ $k_{-1} = 9.11(\pm0.46) \times 10^{-5}$	
0.30 M LiI in $(CD_3)_2CO$	$k_1 = 4.77(\pm0.05) \times 10^{-4}$ k_{-1} = small[a]		
0.50 M LiI in $(CD_3)_2CO$	$k_1 = 6.16(\pm0.04) \times 10^{-4}$ k_{-1} = small[a]	$k_1 = 1.34(\pm0.18) \times 10^{-3}$ $k_{-1} = 1.34(\pm0.18) \times 10^{-4}$	
0.10 M LiOTf in $(CD_3)_2CO$	$k_1 = 5.24(\pm0.20) \times 10^{-4}$ k_{-1} = small[a]	too fast to measure	
0.20 M LiOTf in $(CD_3)_2CO$	$k_1 = 1.12(\pm0.06) \times 10^{-3}$ k_{-1} = small[a]	too fast to measure	
0.50 M LiOTf in $(CD_3)_2CO$	$k_1 = 1.64(\pm0.05) \times 10^{-3}$ k_{-1} = small[a]	too fast to measure	

[a] Insufficient product was present at equilibrium to be detected by NMR measurements.

Scheme 1

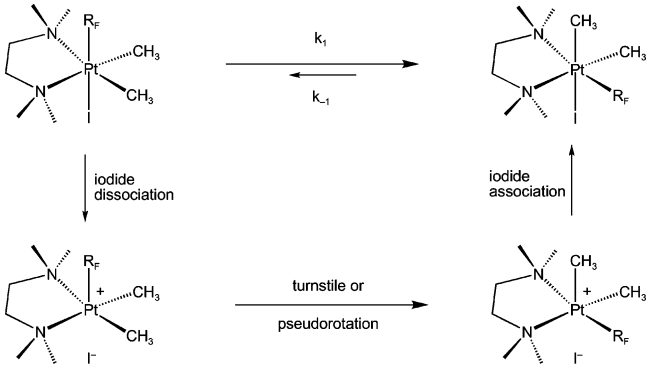

Two mechanisms for isomerization were contemplated. Each is dissociative to afford a 5-coordinate intermediate, either by loss of iodide as shown in Scheme 1, or by an "arm-off" process involving the TMEDA ligand. Rearrangement of the intermediate by Berry pseudorotation or turnstile rotation followed by ligand recombination affords overall *trans* to *cis* isomerization at the metal center.[32,33] This simple isomerization reaction should reflect the kinetic *trans*-effects of the differently fluorinated alkyl ligands provided that iodide dissociation is, or occurs prior to, the rate-limiting step. Loss of iodide from a similar Pt(IV) complex, Pt(DPPE)$(CH_3)_3$I, has been shown to afford a similar 5-coordinate intermediate, from which reductive elimination of CH_3I or C_2H_6 can occur.[34] Under the mild conditions of isomerization observed for these compounds, no such reductive elimination occurs, although more vigorous conditions or longer time periods do result in loss of CH_3I, as previously described.[22] As a result of these competitive reactions, the kinetics of the simple isomerizations can only be studied at or around room temperature. Also notable is the fact that the cationic intermediate initially formed in Scheme 1 is identical to that proposed as the intermediate in the formation of the *trans*-isomers by oxidative addition of R_FI to Pt(TMEDA)$(CH_3)_2$.[22] If this is indeed the case, trapping of this species by iodide must be faster than rearrangement to give the observed *trans*-isomers as the kinetic products of oxidative addition.

The reactions of **12** → **15** and **14** → **17** are stereochemically simpler and are discussed first; isomerization of **13** → **16** is complicated by the formation of two diastereomers of **16** (see below). Both isomerizations were monitored by NMR spectroscopy in deuterated benzene at 21 °C, using trimethoxybenzene as an internal standard. In this solvent, each reaction followed first-order reversible kinetics to form an equilibrium mixture. For **12** → **15** $K_{eq} = 18.1$, with $k_1 = 1.69(\pm0.06) \times 10^{-5}$ s^{-1} and $k_{-1} = 9.37(\pm0.36) \times 10^{-7}$ s^{-1}. For **14** → **17** $K_{eq} = 22.2$, with $k_1 = 5.97(\pm0.54) \times 10^{-5}$ s^{-1} and $k_{-1} = 2.69(\pm0.24) \times 10^{-6}$ s^{-1}. A summary of all rate constants is presented in Table 2.

Each isomerization was also monitored in acetone-d_6. Reaction of **12** → **15** proceeded essentially to completion, to give a solution in which no signals due to **12** could be observed. The reaction was modeled as a first-order nonreversible reaction affording $k = 2.74(\pm 0.01) \times 10^{-4}$ s^{-1}. In contrast, reaction of **14** → **17** followed first-order reversible kinetics, with $K_{eq} = 16.0$ and $k_1 = 6.80(\pm0.25) \times 10^{-4}$ s^{-1} and $k_{-1} = 4.25(\pm 0.16) \times 10^{-5}$ s^{-1}. In addition, the

(26) Monaghan, P. K.; Puddephatt, R. J. *J. Chem. Soc., Dalton Trans.* **1988**, 595−599.
(27) Crespo, M.; Puddephatt, R. J. *Organometallics* **1987**, *6*, 2548−2550.
(28) Jawad, J. K.; Puddephatt, R. J. *J. Chem. Soc., Dalton Trans.* **1977**, 1466−1469.
(29) Jawad, J. K.; Puddephatt, R. J. *J. Organomet. Chem.* **1976**, *117*, 297−302.
(30) Levy, C. J.; Puddephatt, R. J.; Vittal, J. J. *Organometallics* **1994**, *13*, 1559−1560.
(31) Janzen, M. C.; Jennings, M. C.; Puddephatt, R. J. *Inorg. Chem.* **2003**, *42*, 4553−4558.
(32) Springer, C. S., Jr. *J. Am. Chem. Soc.* **1973**, *95*, 1459−1467.
(33) Ugi, I.; Marquarding, D.; Klusacek, H.; Gillespie, P.; Ramirez, F. *Acc. Chem. Res.* **1971**, *4*, 288−296.
(34) Goldberg, K. I.; Yan, J.; Breitung, E. M. *J. Am. Chem. Soc.* **1995**, *117*, 6889−6896.

isomerization of **12** → **15** was also investigated in CD_3NO_2 and DMF-d_7. In each case the isomerization was too fast to monitor at 21 °C and was effectively complete as soon as the sample was placed in the NMR spectrometer. We conclude that the rate limiting step in the mechanism of isomerization is strongly dependent on solvent dielectric constant, favoring loss of iodide to give a polar intermediate, rather than an "arm-off" reaction of the chelate to give a neutral intermediate. Solvent coordinating ability does not appear to be important, as both CD_3NO_2 (poor donor) and DMF-d_7 (good donor) give strongly enhanced rates.[35]

Given that the intermediate is indeed that formed by dissociation of iodide *trans* to the fluoroalkyl ligand as shown in Scheme 1, we can conclude that the rates of isomerization do indeed reflect the kinetic *trans*-effect of the given R_F group. On the basis of the observed k_1 values, the kinetic *trans*-effect of CH_2CF_3 is about three times that of CF_2CF_3 in C_6D_6 or acetone-d_6, reflecting the anticipated difference in σ-donor properties of the alkyl ligands.

More detailed insight into the structure of the intermediate formed by iodide dissociation is revealed by experiments aimed at observing a common ion effect. As mentioned previously, loss of iodide from Pt(DPPE)$(CH_3)_3$I has been shown to afford a 5-coordinate intermediate from which reductive elimination of CH_3I or C_2H_6 can occur.[34,36−39] In this system, the rate of reductive elimination of ethane in acetone is strongly inhibited by added iodide.[34] In contrast, addition of increasing concentrations of LiI to acetone solutions of **12** actually increased the rate of isomerization to give **15** (Table 2). A plot of k_{obs} versus [LiI] is linear (Figure 5). Rates of dissociative reactions that proceed via

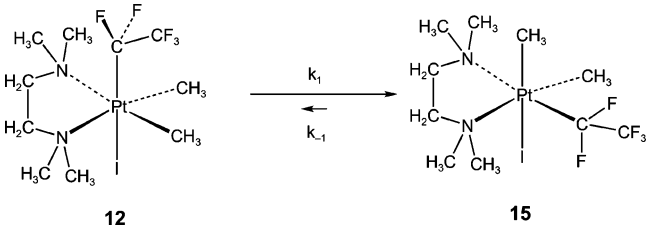

12 **15**

polar intermediates are increased by the addition of ionic salts due to an increased dielectric of the medium.[40] Such systems are characterized by a linear relationship between k_{obs} and salt concentration that can be described in the equation $k_{obs} = k_o(1 + b\{\text{salt}\})$, where k_o is the rate constant in the absence of salt.[40,41] This equation is only strictly valid for first-order nonreversible reactions, as observed for the isomerization of **12** → **15** in acetone. The *b* value is only useful for calculating rates at other salt concentrations for

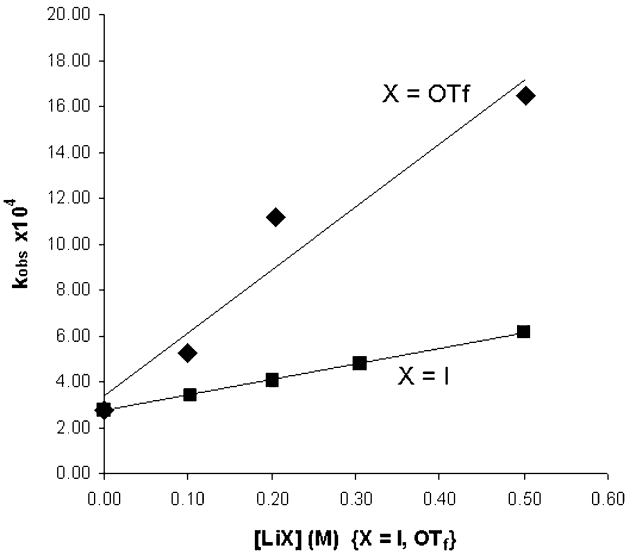

Figure 5. Effect of added lithium salts on the rate constant for isomerization of **12** → **15** in acetone-d_6.

the same reacting system; in this case the *b* value determined from the slope of the graph is 2.5, which falls in the range of reported *b* values.[41] Similar observations were observed when the isomerization of **12** → **15** was carried out in the presence of varying concentrations of a non-common-ion salt, lithium triflate, in acetone (Figure 5). In this case the *b* value is 10.0, which once again falls in the range of reported *b* values. There are three different options for a dissociatively formed ionic intermediate: it can be formed as an intimate ion pair, a solvent separated ion pair, and as dissociated ions.[42] If a common ion is added and there is no solvent separation of the ion pair, i.e., they remain as an intimate ion pair during isomerization, the common ion provides no rate inhibition but follows the normal accelerative salt effect.[42] In other words, the salt effect observed on addition of LiI to the **12** → **15** isomerization follows the pattern expected for an intimate ion pair as interpreted by Winstein for analogous observations on polar dissociative organic reactions,[41−43] or alternatively for rate limiting dissociation of iodide influenced by a large dissolved salt effect on the local dielectric of the medium.

Even though the linear relationship described above is only strictly valid for those reactions that follow a first-order nonreversible reaction mechanism, the conversion of **14** → **17** was also monitored in the presence of varying concentrations of lithium iodide or lithium triflate. Increased rates were

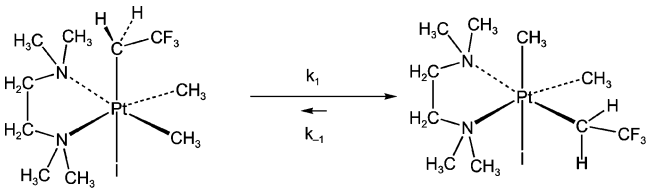

14 **17**

observed, as shown in Table 2. From these results, it is clear that an analogous accelerative salt effect is operative, with

(35) Reichardt, C. *Solvents and Solvent Effects in Organic Chemistry*, 3rd ed.; Wiley-VCH: Weinheim, 2003.
(36) Byers, P. K.; Canty, A. J.; Crespo, M.; Puddephatt, R. J.; Scott, J. D. *Organometallics* **1988**, *7*, 1363−1367.
(37) Hill, G. S.; Puddephatt, R. J. *Organometallics* **1997**, *16*, 4522−4524.
(38) Brown, M. P.; Puddephatt, R. J.; Upton, C. E. E. *J. Chem. Soc., Dalton Trans.* **1974**, 2457−2465.
(39) Brown, M. P.; Puddephatt, R. J.; Upton, C. E. E. *Proc. Int. Conf. Coord. Chem., 16th* **1974**, 3.22, 23 pp.
(40) Lowry, T. H.; Richardson, K. S. *Mechanism and theory in organic chemistry*, 3rd ed.; Harper & Row: New York, 1987.

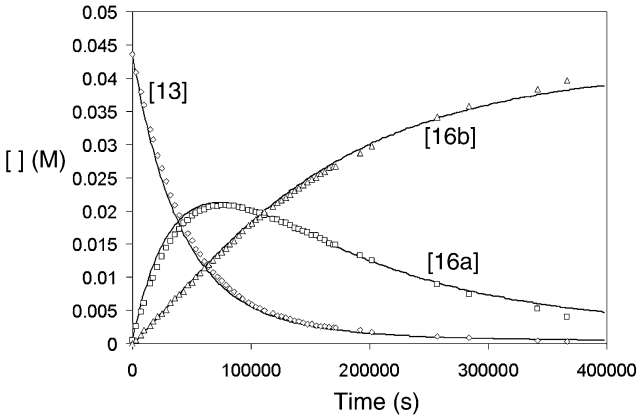

Figure 6. Concentration vs time plot for the isomerization of compound **13** in C_6D_6; experimental data (points) and simulation using the rate constants in Table 2 (solid lines).

the triflate being more effective than the iodide, consistent with results described above for the **12** → **15** isomerization.

Turning now to the case of the isomerization of **13**, increased stereochemical complexity is encountered because the stereocenter at carbon results in two possible diastereomers of the product, **16a** and **16b**, as shown. Fortunately,

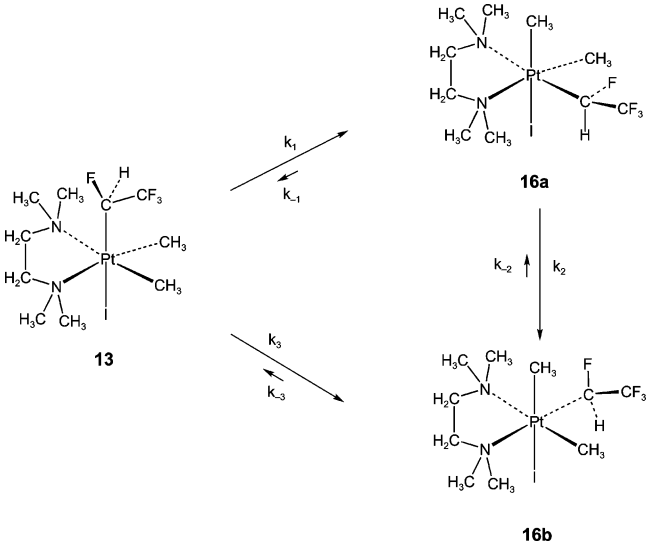

the molecular structures of **13** and the thermodynamic *cis* isomer **16b** have been determined, allowing the relative stereochemistry of the kinetic *cis* isomer **16a** to be established as shown. The molecular structures are described later.

The isomerization of compound **13** was monitored in both C_6D_6 and acetone-d_6 at 21 °C with the internal standard trimethoxybenzene. Figure 6 shows typical results in benzene, with a comparison of experimental data with those obtained by simulation using the rate constants listed in Table 2. As observed in the other systems, isomerization of **13** in acetone-d_6 showed a strong rate enhancement. Accurate equilibrium concentrations could not be determined due to

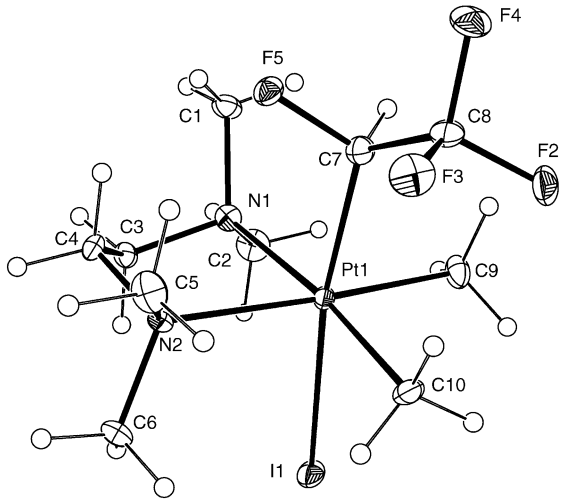

Figure 7. ORTEP diagram of **13**, showing the atom labeling scheme. Thermal ellipsoids are shown at 30% probability. Selected bond lengths (Å) and angles (deg): Pt(1)−C(7) 2.068(5), Pt(1)−C(10) 2.066(5), Pt(1)−C(9) 2.076(5), Pt(1)−N(2) 2.272(4), Pt(1)−N(1) 2.281(4), Pt(1)−I(1) 2.7669(4), C(7)−Pt(1)−C(10) 94.8(2), C(7)−Pt(1)−C(9) 83.4(2), C(10)−Pt(1)−C(9) 90.9(2), C(7)−Pt(1)−N(2) 96.17(17). C(10)−Pt(1)−N(2) 93.25(18), C(9)−Pt(1)−N(2) 175.83(18), C(7)−Pt(1)−N(1) 89.56(18), C(10)−Pt(1)−N(1) 173.94(19), C(9)−Pt(1)−N(1) 93.74(19), N(2)−Pt(1)−N(1) 82.10(14), C(7)−Pt(1)−I(1) 169.87(14), C(10)−Pt(1)−I(1) 85.11(15), C(9)−Pt(1)−I(1) 86.48(15), N(2)−Pt(1)−I(1) 93.95(10), N(1)−Pt(1)−I(1) 91.31(11).

the precipitation of the final product **16b**. Observation that both *cis* diastereomers **16a** and **16b** are present at the beginning of the reaction indicates that both can be formed directly from the *trans*-isomer rather than sequentially forming one *cis*-isomer followed by isomerization to the other. Consequently, the system was modeled using a scheme involving a triangular set of three reversible equilibria.

The rate constants thus determined are shown in Table 2, and on the basis of k_1 values, place the kinetic *trans*-effect of the $CFHCF_3$ group in **13** between that of CF_2CF_3 (**12**) and CH_2CF_3 (**14**). Overall these results are those expected on the basis of σ-donor ability of the three ligands, with stronger σ-donors better stabilizing the cationic transition state.[44]

It is clear from Figure 6 that the rate at which isomer **16a** is formed from **13** significantly exceeds that at which the other diastereomer **16b** is produced, even though **16b** is thermodynamically preferred. A rationale for this observation can be found by examination of the solid-state structures of **13** and **16b** as determined by X-ray crystallography. ORTEP diagrams are provided in Figures 7 and 8, along with selected bond lengths and angles. As with all TMEDA complexes of Pd(II) and Pt(IV) discussed here, and elsewhere,[8,22] the chelate ring is puckered, giving rise to pseudoaxial and equatorial methyl groups on each nitrogen. In the structure of **13** (Figure 7), the axial CH_3 (C1) is *cis* to the $CFHCF_3$ group. If the intermediate cation formed by loss of iodide from **13** has the same conformation within the TMEDA ligand, turnstile rotation of the three alkyl groups should occur preferentially to avoid the bulkier fluoroalkyl group

(41) Fainberg, A. H.; Winstein, S. *J. Am. Chem. Soc.* **1956**, *78*, 2763−2767.
(42) Winstein, S.; Klinedinst, P. E., Jr.; Robinson, G. C. *J. Am. Chem. Soc.* **1961**, *83*, 885−895.
(43) Winstein, S.; Robinson, G. C. *J. Am. Chem. Soc.* **1958**, *80*, 169−181.
(44) Atwood, J. D.; Wovkulich, M. J.; Sonnenberger, D. C. *Acc. Chem. Res.* **1983**, *16*, 350−355.

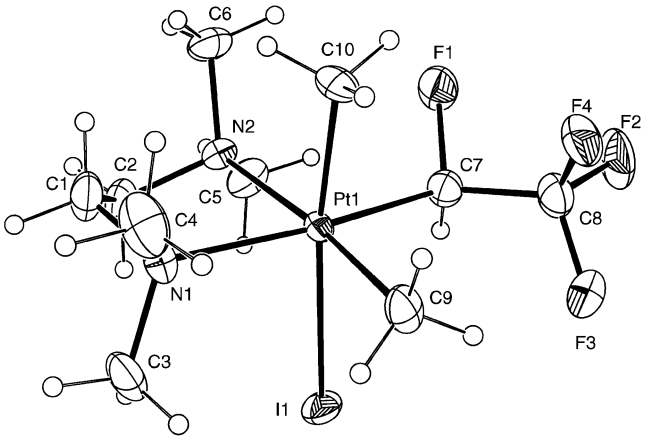

Figure 8. ORTEP diagram of **16b**, showing the atom labeling scheme. Thermal ellipsoids are shown at 30% probability. Selected bond lengths (Å) and angles (deg): Pt(1)−C(7) 2.040(5), Pt(1)−C(10) 2.064(5), Pt(1)−C(9) 2.064(5), Pt(1)−N(1) 2.230(4), Pt(1)−N(2) 2.263(4), Pt(1)−I(1) 2.8048(4), C(7)−Pt(1)−C(10) 88.6(2), C(7)−Pt(1)−C(9) 95.4(2), C(10)−Pt(1)−C(9) 87.9(2), C(7)−Pt(1)−N(1) 173.89(19), C(10)−Pt(1)−N(1) 90.8(2), C(9)−Pt(1)−N(1) 90.7(2), C(7)−Pt(1)−N(2) 91.58(19), C(10)−Pt(1)−N(2) 93.00(19), C(9)−Pt(1)−N(2) 173.0(2), N(1)−Pt(1)−N(2) 82.37(16), C(7)−Pt(1)−I(1) 86.76(17), C(10)−Pt(1)−I(1) 172.82(16), C(9)−Pt(1)−I(1) 87.09(19), N(1)−Pt(1)−I(1) 94.38(12), N(2)−Pt(1)−I(1) 92.63(11).

passing the axial N−CH$_3$; i.e., toward the reader. Thus, the cationic precursor to **16a** should be formed with a lower barrier than that for turnstile rotation in the opposite sense to afford the cationic precursor to **16b**.

Conclusions

There is no evidence for differences in the structural *trans*-influence of alkyl ligands with increased fluorination of the α-carbon atom in square planar complexes of Pd(II) containing the TMEDA ligand. There is a measurable diminution in the kinetic *trans*-effect of alkyl ligands with increasing α-fluorination as observed in the *trans*−*cis* isomerization of octahedral Pt(IV) complexes, in which the *trans*-effect follows the order R$_F$ = CH$_2$CF$_3$ > CFHCF$_3$ > CF$_2$CF$_3$. The mechanism of isomerization involves iodide dissociation to give an intimate ion-pair with no apparent solvent separation.

Experimental Section

General Considerations. Unless otherwise noted, all reactions were performed in oven-dried glassware, using standard Schlenk techniques, under an atmosphere of nitrogen, which had been deoxygenated over BASF catalyst and dried using Aquasorb. Solvents were deoxygenated and dried over activated alumina using an apparatus modified from that described in the literature.[45] ^{1}H (300 or 500 MHz), ^{19}F (282 MHz), and ^{31}P (121.4 MHz) NMR spectra were recorded on Varian Unity Plus spectrometers. Chemical shifts are reported as ppm downfield of TMS (^{1}H, referenced to solvent) or internal CFCl$_3$ (^{19}F). Coupling constants are reported in Hertz (Hz). Microanalyses were performed by Schwartzkopf Microanalytical Laboratory (Woodside, NY).

CF$_3$CF$_2$I and CF$_3$CH$_2$I were purchased from Lancaster, and CF$_3$CFHI from ABCR. Each was treated with Na$_2$S$_2$O$_3$ to remove residual I$_2$, and vacuum distilled before use. The complexes Pd(TMEDA)(CH$_3$)$_2$ and Pt(TMEDA)(CH$_3$)$_2$ were prepared by literature methods.[46−48]

Pd(TMEDA)(CF$_2$CF$_3$)(CH$_3$) (9). To a suspension of Pd(TMEDA)(CH$_3$)$_2$ (0.099 g, 0.392 mmol) in hexanes (20 mL) was added CF$_3$CF$_2$I (0.4 g, 1.6 mmol). The mixture was stirred overnight at room temperature in the absence of light. The resulting yellow suspension was filtered and washed with warm hexanes (3 × 10 mL). The yellow filtrate was collected, and the volatiles were removed in vacuo to yield a yellow crystalline solid (0.062 g, 0.172 mmol, 44%). Anal. Calcd for C$_9$H$_{19}$F$_5$N$_2$Pd: C 30.31, H 5.37. Found: C 30.04, H 5.30%. ^{1}H NMR (C$_6$D$_6$, 300 MHz, 23 °C): δ 0.67 (tq, $^4J_{HF}$ = 1 Hz, $^5J_{HF}$ = 1 Hz, 3H, PdCH$_3$), 1.39−1.41 (m, 4H, CH$_2$CH$_2$), 1.65 (s, 6H, NCH$_3$), 2.09 (s, 6H, NCH$_3$). ^{19}F NMR (C$_6$D$_6$, 282.2 MHz, 23 °C): δ −97.8 (br s, CF$_2$), −80.9 (br s, CF$_3$).

Pd(TMEDA)(CFHCF$_3$)(CH$_3$) (10). To a suspension of Pd(TMEDA)(CH$_3$)$_2$ (0.078 g, 0.310 mmol) in hexanes (20 mL) was added CF$_3$CFHI (0.04 mL, 0.35 mmol). The mixture was stirred overnight at room temperature. The resulting yellow suspension was filtered and washed with warm hexanes (3 × 10 mL). The yellow filtrate was collected, and the volatiles were removed in vacuo to yield a pale yellow crystalline solid (0.056 g, 0.167 mmol, 54%). Anal. Calcd for C$_9$H$_{20}$F$_4$N$_2$Pd: C 31.92, H 5.95. Found: C 31.59, H 5.86%. ^{1}H NMR (C$_6$D$_6$, 300 MHz, 23 °C): δ 0.31 (q, $^5J_{HF}$ = 1 Hz, 3H, PdCH$_3$), 1.21−1.34 (m, 2H, CH$_2$), 1.61−1.74 (m, 2H, CH$_2$), 1.72 (s, 3H, NCH$_3$), 1.77 (s, 3H, NCH$_3$), 2.09 (s, 3H, NCH$_3$), 2.31 (s, 3H, NCH$_3$), 6.01 (dq, $^2J_{HF}$ = 50 Hz, $^3J_{HF}$ = 13 Hz, 1H, CH). ^{19}F NMR (C$_6$D$_6$, 282.2 MHz, 23 °C): δ −220.0 (dq, $^2J_{FH}$ = 50 Hz, $^3J_{FF}$ = 13 Hz, CF), −68.0 (dd, $^3J_{FF}$ = 13 Hz, $^3J_{FH}$ = 13 Hz, CF$_3$).

Pd(TMEDA)(CH$_2$CF$_3$)(CH$_3$) (11). To a suspension of Pd(TMEDA)(CH$_3$)$_2$ (0.122 g, 0.484 mmol) in Et$_2$O (20 mL) was added CF$_3$CH$_2$I (0.05 mL, 0.51 mmol). The mixture was stirred overnight at room temperature in the absence of light. The resulting yellow suspension was filtered and washed with warm hexanes. The yellow filtrate was collected, and the volatiles were removed in vacuo to yield a pale yellow crystalline solid (0.071 g, 0.223 mmol, 46%). Anal. Calcd for C$_9$H$_{21}$F$_3$N$_2$Pd: C 33.71, H 6.60. Found: C 33.62, H 6.67%. ^{1}H NMR (C$_6$D$_6$, 300 MHz, 23 °C): δ 0.58 (m, 3H, PdCH$_3$), 1.47 (s, 4H, CH$_2$CH$_2$) 1.60 (q, $^3J_{HF}$ = 17 Hz, 2H, PdCH$_2$), 1.81 (s, 3H, NCH$_3$), 1.90 (s, 3H, NCH$_3$). ^{19}F NMR (C$_6$D$_6$, 282.2 MHz, 23 °C): δ −47.3 (t, $^3J_{FH}$ = 17 Hz, CF$_3$).

***trans*-Pt(TMEDA)(CF$_2$CF$_3$)(CH$_3$)$_2$I (12).** To a suspension of Pt(TMEDA)(CH$_3$)$_2$ (300 mg, 0.878 mmol) in toluene (20 mL) at −78 °C was added CF$_3$CF$_2$I (0.4 g, 1.64 mmol). The solution immediately turned yellow in color. The reaction mixture was stirred for approximately 5 min, and the solvent was removed in vacuo while maintaining the temperature below 0 °C. A light yellow solid was obtained in quantitative yield and was stored at −35 °C. ^{1}H NMR (C$_6$D$_6$): δ 2.73 (s, 6H, $^3J_{PtH}$ = 13 Hz, NCH$_3$), 2.16 (m, 2H, NCH$_2$), 2.10 (tq, 6H, $^4J_{FH}$ = 1 Hz, $^5J_{FH}$ = 1 Hz, $^2J_{PtH}$ = 70 Hz, PtCH$_3$), 2.02 (s, 6H, $^3J_{PtH}$ = 12 Hz, NCH$_3$), 1.86 (m, 2H, NCH$_2$) ppm.^{19}F NMR (C$_6$D$_6$): δ −78.10 (s, $^3J_{PtF}$ = 14 Hz, CF$_3$), −90.66 (s, $^2J_{PtF}$ = 223 Hz, CF$_2$) ppm. The compound isomerizes to the *cis* isomer **15** on standing in solution.

***cis*-Pt(TMEDA)(CF$_2$CF$_3$)(CH$_3$)$_2$I (15).** To a suspension of (TMEDA)Pt(CH$_3$)$_2$ (0.100 g, 0.293 mmol) in hexanes (20 mL) was added CF$_3$CF$_2$I (0.2 g, 0.82 mmol). The mixture was stirred overnight at room temperature in the absence of light. The resulting pale yellow suspension was filtered, and the residue was washed

(45) Pangborn, A. B.; Giardello, M. A.; Grubbs, R. H.; Rosen, R. K.; Timmers, F. J. *Organometallics* **1996**, *15*, 1518−1520.

(46) Monaghan, P. K.; Puddephatt, R. J. *Organometallics* **1984**, *3*, 444−449.

(47) Yang, D. S.; Bancroft, G. M.; Dignard-Bailey, L.; Puddephatt, R. J.; Tse, J. S. *Inorg. Chem.* **1990**, *29*, 2487−2495.

(48) de Graaf, W.; Boersma, J.; Smeets, W. J. J.; Spek, A. L.; van Koten, G. *Organometallics* **1989**, *8*, 2907−2917.

with hexanes (3 × 5 mL). The solid was recrystallized from CH_2Cl_2/hexanes. The pale yellow solid was collected and dried in vacuo (0.143 g, 0.243 mmol, 83%). Anal. Calcd for $C_{10}H_{22}F_5IN_2Pt$: C 20.45, H 3.78. Found: C 20.60, H 3.64%. ^{1}H NMR (C_6D_6, 300 MHz, 23 °C): δ 1.09 (d, $^2J_{HPt}$ = 64 Hz, $^4J_{HF}$ = 2 Hz, 3H, $PtCH_3$), 1.34−1.55 (m, 2H, CH_2), 1.39 (s, $^3J_{HPt}$ = 18 Hz, 3H, NCH_3), 1.82 (s, $^2J_{HPt}$ = 70 Hz, 3H, $PtCH_3$), 1.87 (s, $^3J_{HPt}$ = 13 Hz, 3H, NCH_3), 1.97−2.18 (m, 2H, CH_2), 2.74 (s, $^3J_{HPt}$ = 15 Hz, 3H, NCH_3), 3.01 (s, $^3J_{HPt}$ = 10 Hz, 3H, NCH_3). ^{19}F NMR (C_6D_6, 282.2 MHz, 23 °C): δ −83.7 (d, $^2J_{FPt}$ = 331 Hz, $^2J_{FF}$ = 252 Hz, CF), −77.3 (s, CF_3), −70.2 (d, $^2J_{FF}$ = 252 Hz, $^2J_{FPt}$ = 245 Hz, CF).

***trans*-Pt(TMEDA)(CFHCF$_3$)(CH$_3$)$_2$I (13).** To a solution of Pt(TMEDA)Me_2 (164 mg, 0.480 mmol) in toluene (15 mL) at −78 °C was added CF_3CFHI (0.06 mL, 0.54 mmol) to produce a pale yellow solution. The solution was warmed to room temperature, and the solvent was then removed in vacuo as quickly as possible. A white solid was obtained in quantitative yield. X-ray quality crystals were grown from toluene/hexane at −30 °C. The compound isomerizes in solution. ^{1}H NMR (C_6D_6, 500 MHz, 21 °C): δ 1.56 (s, $^2J_{HPt}$ = 67.5 Hz, 3H, PtMe), 1.54−1.59 (m, 1H, CH_2), 1.65 (s, $^3J_{HPt}$ = 11.0 Hz, 3H, NMe), 1.67−1.71 (m, 1H, CH_2), 1.98−2.04 (m, 1H, CH_2), 2.11 (q, $^5J_{HF}$ = 2.0 Hz, $^2J_{HPt}$ = 71.0 Hz, 3H, PtMe), 2.12 (s, $^3J_{HPt}$ = 14.0 Hz, 3H, NMe), 2.32−2.37 (m, 1H, CH_2), 2.69 (s, $^3J_{HPt}$ = 12.0 Hz, 3H, NMe), 2.72 (s, $^3J_{HPt}$ = 13.0 Hz, 3H, NMe), 5.17 (dq, $^2J_{HF}$ = 46.5 Hz, $^3J_{HF}$ = 10.0 Hz, $^2J_{HPt}$ = 85.0 Hz, 1H, $CFHCF_3$). ^{19}F NMR (C_6D_6, 470.4 MHz, 21 °C): δ −187.4 (dq, $^2J_{FH}$ = 46.5 Hz, $^3J_{FF}$ = 11.0 Hz, $^2J_{FPt}$ = 164.5 Hz, C*F*HCF$_3$), −68.8 (br, CFHC*F*$_3$).

***cis*-Pt(TMEDA)(CFHCF$_3$)(CH$_3$)$_2$I (16a and 16b).** A sample of **13** (17 mg, 0.030 mmol) was dissolved in C_6D_6 and allowed to stand at room temperature for 2 weeks. A solution containing 94.8% **16b**, 4.8% **16a**, and 0.4% **13** was obtained. The solvent was removed and the solid residue recrystallized from CH_2Cl_2/heptane to yield X-ray quality crystals of **16b**. Anal. Calcd for $C_{10}H_{23}F_4IN_2Pt$: C 21.10, H 4.07. Found: C 21.26, H 4.02%. NMR (**16a**) ^{1}H NMR (C_6D_6, 500 MHz, 21 °C): δ 0.79 (d, $^4J_{HF}$ = 1.0 Hz, $^2J_{HPt}$ = 64.0 Hz, 3H, PtMe), 1.32−1.37 (m, 2H, CH_2), 1.37 (s, $^3J_{HPt}$ = 17.0 Hz, 3H, NMe), 1.68 (s, $^2J_{HPt}$ = 69.0 Hz, 3H, PtMe), 1.70 (s, $^3J_{HPt}$ = 12.5 Hz, 3H, NMe), 1.90−1.97 (m, 2H, CH_2), 2.69 (s, $^3J_{HPt}$ = 14.5 Hz, 3H, NMe), 2.89 (s, $^3J_{HPt}$ = 10.5 Hz, 3H, NMe), 6.10 (dq, $^2J_{HF}$ = 46.5 Hz, $^3J_{HF}$ = 10.0 Hz, $^2J_{HPt}$ = 72.0 Hz, 1H, $CFHCF_3$). ^{19}F NMR (C_6D_6, 470.4 MHz, 21 °C): δ −185.3 (br, dq, $^2J_{FH}$ = 47.0 Hz, $^3J_{FF}$ = 11.0 Hz, $^2J_{FPt}$ = 250.0 Hz, C*F*HCF$_3$), −69.4 (dd, $^3J_{FF}$ = 11.0 Hz, $^3J_{FH}$ = 10.0 Hz, $^3J_{FPt}$ = 59.0 Hz, CFHC*F*$_3$). NMR (**16b**) ^{1}H NMR (C_6D_6, 500 MHz, 21 °C): δ 1.13 (s, $^2J_{HPt}$ = 66.0 Hz, 3H, PtMe), 1.35−1.40 (m, 1H, CH_2), 1.42 (s, $^3J_{HPt}$ = 18.0 Hz, 3H, NMe), 1.54−1.62 (m, 2H, CH_2), 1.73 (q, $^5J_{HF}$ = 1.5 Hz, $^2J_{HPt}$ = 69.0 Hz, 3H, PtMe), 1.77 (s, $^3J_{HPt}$ = 13.0 Hz, 3H, NMe), 2.55−2.61 (m, 1H, CH_2), 2.71 (s, $^3J_{HPt}$ = 13.5 Hz, 3H, NMe), 2.90 (s, $^3J_{HPt}$ = 10.5 Hz, 3H, NMe), 7.54 (dq, $^2J_{HF}$ = 47.0 Hz, $^3J_{HF}$ = 10.0 Hz, $^2J_{HPt}$ = 115.0 Hz, 1H, $CFHCF_3$). ^{19}F NMR (C_6D_6, 470.4 MHz, 21 °C): δ −190.4 (dq, $^2J_{FH}$ = 47.0 Hz, $^3J_{FF}$ = 12.0 Hz, $^2J_{FPt}$ = 234.0 Hz, C*F*HCF$_3$), −69.7 (dd, $^3J_{FF}$ = 11.0 Hz, $^3J_{FH}$ = 10.0 Hz, $^3J_{FPt}$ = 60.0 Hz, CFHC*F*$_3$).

***trans*-Pt(TMEDA)(CH$_2$CF$_3$)(CH$_3$)$_2$I (14).** To a suspension of Pt(TMEDA)$(CH_3)_2$ (240 mg, 0.703 mmol) in toluene (20 mL) at −78 °C was added CF_3CH_2I (0.12 mL, 1.22 mmol). The solution immediately turned yellow in color. The reaction mixture was stirred for approximately 10 min, and the solvent was removed in vacuo while maintaining the temperature below 0 °C. A white solid was obtained in quantitative yield and was stored at −35 °C. The complex isomerizes to the *cis*-isomer **17** in solution. ^{1}H NMR (C_6D_6): δ 2.79 (s, 6H, $^3J_{PtH}$ = 11 Hz, NCH_3), 2.12−2.01 (m, 2H, NCH_2), 1.98 (d, 6H, $^5J_{FH}$ = 1 Hz, $^2J_{PtH}$ = 71 Hz, $PtCH_3$), 1.75 (q, 2H, $^3J_{FH}$ = 14 Hz, $^2J_{PtH}$ = 100 Hz, CH_2CF_3), 1.51 (s, 6H, $^3J_{PtH}$ = 13 Hz, NCH_3), 1.46−1.35 (m, 2H, NCH_2) ppm. ^{19}F NMR (C_6D_6): δ −53.22 (t, $^3J_{FH}$ = 14 Hz, $^3J_{PtF}$ = 108 Hz, CH_2CF_3) ppm.

***cis*-Pt(TMEDA)(CH$_2$CF$_3$)(CH$_3$)$_2$I (17).** To a suspension of Pt(TMEDA)$(CH_3)_2$ (0.124 g, 0.363 mmol) in hexanes (20 mL) was added CF_3CH_2I (0.05 mL, 0.51 mmol). The mixture was stirred overnight at room temperature in the absence of light. The resulting white suspension was filtered, and the residue was washed with hexanes (3 × 5 mL). The solid was recrystallized from CH_2Cl_2/hexanes. The white solid was collected and dried in vacuo (0.178 g, 0.323 mmol, 89%). Anal. Calcd for $C_{10}H_{24}F_3IN_2Pt$ (551.29): C 21.79, H 4.39. Found: C 22.03, H 4.47. ^{1}H NMR (C_6D_6, 300 MHz, 23 °C): δ 0.90 (q, $^2J_{FH}$ = 0.6 Hz, $^2J_{HPt}$ = 66 Hz, 3H, $PtCH_3$), 1.37−1.58 (m, 2H, CH_2), 1.46 (s, $^3J_{HPt}$ = 19 Hz, 3H, NCH_3), 1.54 (s, $^3J_{HPt}$ = 14 Hz, 3H, NCH_3), 1.82 (q, $^2J_{HPt}$ = 69 Hz,$^4J_{HH}$ = 0.6 Hz, 3H, $PtCH_3$), 1.82−1.92 (m, 1H, CH_2), 2.07−2.19 (m, 1H, CH_2), 2.53 (dq, $^2J_{HPt}$ = 100 Hz, $^2J_{HH}$ = 15 Hz, $^3J_{HF}$ = 14 Hz, 1H, $PtCH_2$), 2.67 (s, $^3J_{HPt}$ = 10 Hz, 3H, NCH_3), 2.77 (s, $^3J_{HPt}$ = 14 Hz, 3H, NCH_3), 3.82 (dq, $^2J_{HPt}$ = 103 Hz, $^2J_{HH}$ = 15 Hz, $^3J_{HF}$ = 13 Hz, 1H, $PtCH_2$). ^{19}F NMR (C_6D_6, 282.2 MHz, 23 °C): δ −53.7 (t, $^2J_{FPt}$ = 107 Hz, $^3J_{FH}$ = 15 Hz, CF_3).

Kinetic Studies. The isomerization reactions were followed in the probe of a Varian Unity Plus 500 Spectrometer at 21 °C with (1,3,5)-trimethoxybenzene as an internal integration standard for all reactions. The T_1 values of all the platinum complexes were checked to ensure full relaxation and accurate reflection of concentration values from integration. Each starting complex was dissolved to 1.00 mL of solution in a volumetric flask, and a sample was transferred to a Young's NMR tube, sealed to avoid solvent evaporation, and placed in the NMR probe. Starting concentrations ranged from 0.065 to 0.054 M. Concentration versus time data were obtained from 3−5 samples of each run. Solutions of varying concentrations of lithium iodide and lithium triflate were weighed and dissolved in acetone-d_6 in a Braun glovebox in volumetric flasks.

X-ray Crystal Structure Determinations. Diffraction intensity data were collected with a Siemens P4/CCD (**9**−**11, 16b**) and a Bruker Smart Apex CCD (**13**) diffractometers. Crystal, data collection, and refinement parameters are given in Table 1. The structures were solved using direct methods, completed by subsequent difference Fourier syntheses, and refined by full matrix least-squares procedures on F^2. SADABS[49,50] absorption corrections were applied to all data. All non-hydrogen atoms were refined with anisotropic displacement coefficients, and hydrogen atoms were treated as idealized contributions. All software and sources scattering factors are contained in the SHELXTL (5.10) program package (G.Sheldrick, Bruker XRD, Madison, WI).

Acknowledgment. R.P.H. is grateful to the National Science Foundation for financial support. We are grateful to Professor Robert Ditchfield for help and insight in the kinetic simulations.

Supporting Information Available: Tables listing crystal data and structural refinement, final atomic coordinates, bond lengths and angles, hydrogen atom positions, and anisotropic thermal parameters (CIF). This material is available free of charge via the Internet at http://pubs.acs.org.

IC030251J

(49) Walker, N.; Stuart, D. *Acta Crystallogr., Sect. A.* **1983**, *39*, 158−166.
(50) Sheldrick, G. M. *SADABS (2.01) Bruker/Siemens Area Detector Absorption Correction Program*; Bruker AXS: Madison, WI, 1998